Experimental tests for the assessment of residual strength of r.c. structures after fire – Case study

Giada Frappa *, Margherita Pauletta, Caterina Di Marco, Gaetano Russo

Polytechnic Department of Engineering and Architecture, University of Udine, Via delle Scienze 206, 33100 Udine, Italy

ARTICLE INFO

Keywords:
Fire
Damage
Concrete
Structural health assessment
Tests
Deteriorated concrete depth
Discs

ABSTRACT

A fire in a ham factory in San Daniele del Friuli caused serious damage to the prefabricated reinforced concrete (r.c.) roof panels and smaller damages to beams, columns and walls. In this paper the data captured during preliminary inspection of the building structure are described. To determine the residual strength of steel reinforcements and concrete of r.c. structural elements, a test program with laboratory and in situ tests is presented. The program includes test methods that are able to catch the variability of concrete degradation with distance from the heated surface. Test results are presented and their acceptability in relation to Italian Code is discussed. It is found that the amount of transversal and longitudinal reinforcements strongly influences the deterioration of the concrete due to fire and, consequently, the strength of structural elements. On the basis of tests results, a discussion on the advantages and limitations of the adopted test methods useful for the designers is performed. To restore the load-bearing capacity of the structure, repairs of columns and beams in the first three bays of the central frame are proposed together with the substitution of the roof over the receiving area.

1. Introduction

When a r.c. building is exposed to fire, one of the main difficulties is the assessment of the residual strength of structural elements. Due to the low thermal conductivity of concrete, the heat flow in heated r.c. elements is strongly non-stationary, producing high temperature gradients within the elements' cross-sections. Concrete damage occurs mainly in the elements' surface layers, which are directly exposed to the fire, and decreases with depth [1–3].

However, as reported by Malešev et Radonjanin [4], in the presence of high temperature gradients, large tensile stresses arise between the fire-affected layers and the colder inner core, leading to the onset of internal cracks, which form parallel to the heated surface of the elements. These cracks are very dangerous, as they evince delamination of the outer layers from the inner core, but they do not appear on the surface. Thus, they cannot be detected by visual inspection.

In order to establish if the structure can be conveniently restored or repaired instead of being demolished, it is important to identify, through experimental tests, the depth of deteriorated concrete in the elements' cross-sections and the concrete residual strength. The design of strengthening should be based on the extent of deterioration beneath the surface.

In the literature many studies [1–3] and [5–8] deal with the experimental tests that can be carried out to assess the damage in r.c. buildings after exposure to fire. These studies describe various laboratory and in situ methods, destructive and non-destructive tests. In order to contain the costs and, at the same time, get the adequate information about structural health and safety, it is crucial to perform tests that provide complete and reliable detection of structural damage.

This paper aims to highlight the advantages and limitations of some tests proposed in the literature. To do so, a number of these tests are used to assess the residual strength of structural elements of an industrial building that suffered a severe fire. Finally, the obtained experimental results are presented and discussed. On the basis of tests results, the authors provide suggestions useful for the interpretation of performed tests.

2. Case study

The building considered herein is a ham factory in San Daniele del Friuli, built in 2004. It is a one-storey complex, composed of a main building with r.c. construction, and two smaller steel frame sheds. The

* Corresponding author.
E-mail addresses: giada.frappa@uniud.it (G. Frappa), margherita.pauletta@uniud.it (M. Pauletta), dimarco.caterina@spes.uniud.it (C. Di Marco), gaetano.russo@uniud.it (G. Russo).

Accepted 27 November 2021

building plan is shown in Fig. 1. The main building comprises a processing plant, which is about 5 m high, and the adjacent office building and changing room, which are 2.5 m high. The steel sheds are labelled as the tailings storage and delivery area, respectively.

The complex has a rectangular floor plan, whose dimensions are approximately 24x38 m. The r.c. structure is composed of long exterior walls with a few columns along the perimeter, and an interior frame parallel to the longitudinal direction of the building. Frame columns have a square section of side 40 cm, while beams have a 40x100 cm rectangular cross-section.

The roof system is a r.c. one-way joist floor with Expanded Poly-Styrene (EPS) lightning blocks, cast in place on the top of prefabricated prestressed r.c. panels, 5 cm thick. The floor has a 7 cm topping slab and 22x45 cm joists, with the axial distance between the joists 60 cm. Joists are oriented parallel to the transverse direction of the building plan.

The data on the dimensions of structural elements, the strength class of concrete and steel reinforcement, as well as the amount and arrangement of the reinforcement in the structural elements were available from design documentation. The concrete strength is classified C25/30 (characteristic cube compressive strength of concrete $R_{ck} = 30$ MPa), and steel reinforcement is of Italian grade FeB 44 k (characteristic yield strength $f_{yk} = 430$ MPa). Concrete in prefabricated r.c. panels is classified C35/45.

As shown in Fig. 1, the complex is divided into two parts by frame infill panels, having fire resistance class REI 120. When viewed from the main entrance, the right side of the building was used for ham curing, while the left side was for deboning.

In the deboning department a 12 cm thick masonry partition wall divided the deboning area from the receiving areas.

The inside surfaces of vertical structural elements (i.e., walls and columns), infill walls, and the intrados of the roof were wrapped with insulating panels.

The fire that broke out in March of 2020 started in the receiving area, where a large amount of flammable materials (hams, wooden pallets, and cardboard packages) were stored. The fire lasted for about two hours and was extinguished with water by firefighters.

3. Preliminary inspection

Before developing a test program, it is fundamental to make a visual inspection of the structure. This assessment, although it may provide only a rough and partial insight of structural damage, is important to identify what are likely the most damaged elements, and, thus, calibrate the test program, determining the desired locations of tests and their number.

During the inspection at the construction site, it was observed that the most damaged area was the receiving zone, where the greatest volume of fire load was stored. In particular, the most severely damaged elements of the load-bearing structure appeared to be the prefabricated r.c. panels of the roof over the receiving zone. Large portions of concrete had fallen off, laying bare the reinforcements along the whole surface of the roof (Fig. 2). Moreover, the adhesion between reinforcements and concrete was visibly impaired. The panel depth affected by concrete spalling often exceeded the cover, and, in some parts, spalling depth was equal to the panel thickness. Reinforcement buckling occurred as well.

The insulating panels on the structural and infill walls and on the frame were visibly deformed and burnt by high temperatures. In some areas, the large deformations caused the panels to detach from their supports.

Fire damage gradually decreased from the receiving to the deboning area, and was substantially less severe in the delivery zone in the external steel shed. Notably, insulating panels were still mostly present in the deboning area roof, and no apparent structural damage was observed. However, beams and columns uncovered by detached panels were darkened by smoke, making it quite difficult to detect any structural damage. Conversely, in the steel sheds, in the office building, and in the changing room no structural damage was recorded. This was due both to the masonry partition wall, which contained the flames mainly

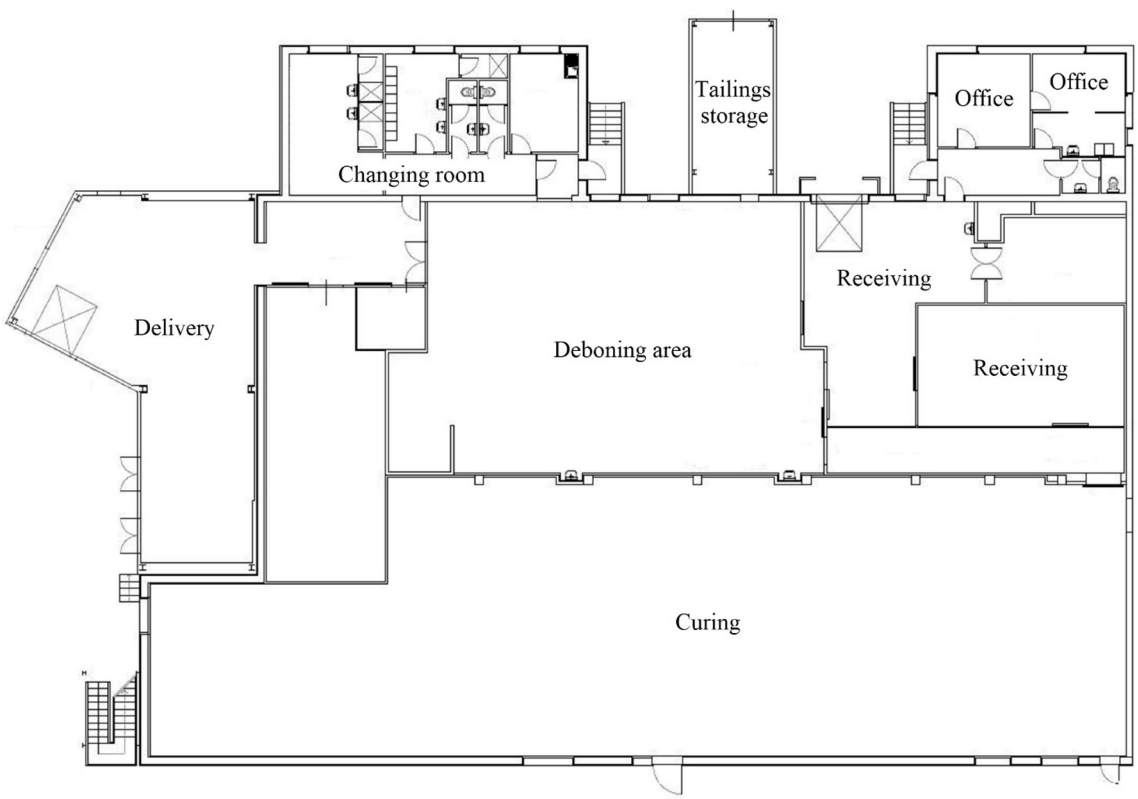

Fig. 1. Building plan.

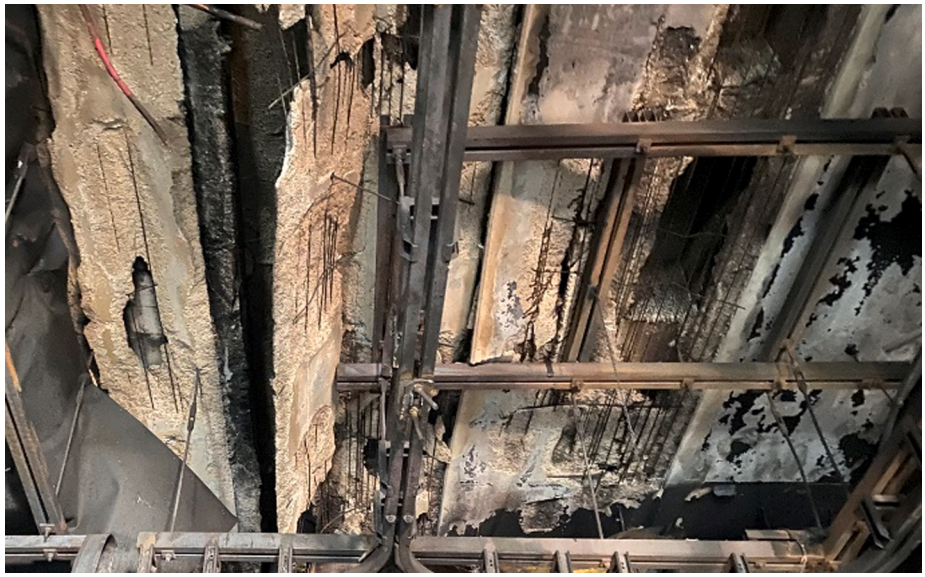

Fig. 2. Damage caused by fire in the prefabricated panels of the roof over the receiving zone.

in the receiving area, and to the presence of a smaller fire load in these areas.

No structural damage was observed in the curing department.

In order to guarantee a complete assessment, under safe conditions, of structural damages caused by the fire, the roof over the receiving area was demolished, and infill and partition walls, insulating panels, and tiles were removed.

Then the bare structure was washed with a high pressure water jet. It is worth noting that hydro-washing does not remove the discoloration due to smoke. Consequently, any colour change of the heated concrete due to the dehydration of the cement paste and the oxidation of mineral components within the aggregate [9] cannot be detected visually on the surface of elements blackened by smoke.

In the receiving area, on the columns and beams of the interior frame and on the adjacent exterior wall, changes in the concrete colour were recorded. More precisely, a pink-red discoloration marred the greater part of the surface of the wall and the adjacent beam of the frame, while on the columns the pink discoloration was less intense and appeared only on the upper part, which was evidently the area exposed to the highest temperatures. As mentioned in [9], the pink-red discoloration is observed in concrete containing siliceous aggregate heated to between 300 °C and 600 °C, due to the dehydration or oxidation of iron compounds in this temperature range.

Moreover, on the interior frame elements, net-like superficial cracks were observed. This type of damage, known as crazing, is due to shrinkage of the cement paste as a result of drying, induced by high temperatures. These cracks were oriented in both the vertical and the horizontal directions. Larger cracks along the edges of the most damaged columns (Fig. 3) and beams, mainly oriented along the longitudinal reinforcement, were observed. These cracks are related to splitting induced by the expansion of steel bars and to the difference between the thermal expansion coefficients of concrete and steel. Despite the presence of splitting cracks, no concrete cover falling off was observed in the frame elements.

To detect the presence of delamination and damage in the outer concrete layer, a hammer was used. In the receiving area, low frequency sounds were recorded in some columns and beams, indicating the presence of weak and friable concrete. Spalling of the concrete cover occurred in some columns and beams in the receiving area.

By visual inspection, splitting cracks around the reinforcement and internal cracks parallel to the fire-exposed surfaces were ascertained. Moreover, in column cross-sections, the chromatic change of concrete

Fig. 3. Splitting cracks around reinforcements in a column in the receiving area.

occurred up to a depth of about 3–4 cm, as it can be observed in Fig. 4.

This observation, although subjective, is useful for estimating the depth of heat penetration in element cross-sections, i.e., the thickness of concrete subjected to temperatures between 300 °C and 600 °C. For a more accurate and objective analysis of the chromatic changes in the concrete, and, consequently, of temperature distribution within the cross-section, a computerized colorimetric analysis based on digital images is suggested. Details can be found in [10].

4. Tests program and results

The visual inspection is useful for detecting changes that can be seen from the outside, typically in the most severely damaged structural elements. But, in less damaged elements, there may be no visible change. Thus, laboratory and in situ tests are necessary to allow a more accurate assessment of the concrete and reinforcement.

The aim of the test program is quantifying the residual strength of steel reinforcements and concrete in damaged r.c. structural elements. In order to optimise the arrangement and location of survey points, a preliminary mapping of the damage distribution within the structure was carried out.

In addition, since fire damage in concrete is more severe in the external layers of the member cross-section, it is important to determine the thickness of deteriorated concrete in order to refine the design of repair intervention.

Fig. 5 shows the locations of survey spots in the building plan. Each spot is labelled by one or two letters identifying the test method: rebound hammer (RH), drilled core (C), or reinforcement sample (S), as indicated in the caption of Fig. 5. The letter(s) is (are) followed by the design cube compressive strength of concrete: 30 for tests on C25/30 and 45 for tests on C35/45 concrete, and by a progressive number, identifying the position.

Fig. 4. Measurement of the in-depth penetration of visible chromatic changes in a concrete fragment detached from a column.

4.1. Concrete

The most significant concrete mechanical property to be determined is compressive strength. The most reliable way to determine it is through destructive testing. Thus, the extraction of drilled cores is considered. Moreover, when dealing with structures subjected to fire, it is imperative to choose test methods that are able to reveal the variability of concrete degradation with the distance from the heated surface. Various tests are presented in the literature on small size specimens [1], [3] and [8] test methods described in [3] and [8] are herein considered. Both methods use thin discs for the determination of compressive [8] and tensile strength [3] of concrete.

Quantity and locations of survey spots are chosen with the purpose of capture the damage variability in concrete strength caused by fire. Test locations are marked in Fig. 5. Tests were performed both on the r.c. elements directly exposed to flames or high temperature and on elements that did not appear to be affected by fire, taken as reference for the original state of elements.

4.1.1. Schmidt rebound hammer

This non-destructive test is used to get an estimation of the compressive strength of concrete in surface layers about 30 mm thick, by measuring surface hardness. Conversely, drilled cores can be used to test the compression strength of concrete along the core height, which is greater than the thickness of the layer detected by sclerometer (Schmidt hammer). In structures not affected by fire, acceptable estimations of the compressive strength may be obtained by making drilled cores and performing sclerometric tests close to core drilling locations, then relating rebound index values to strength of drilled cores and using the obtained relationship to estimate the concrete compressive strength in other locations tested only with the sclerometer. By contrast, the surface layer of fire-damaged concrete has a lower rebound index than that of undamaged concrete [11], while the compressive strength of drilled cores benefits from the structural integrity of the inner core, which is less damaged than the cover. This difference could lead to unsafe correlations between rebound index and concrete compression strength in fire-damaged concrete, as referred in [2] and [11].

However, in fire-damaged structures, the sclerometric test can be conveniently used for mapping the damage distribution in the structure. By considering a sufficient number of survey points and comparing values of rebound index, zones vith varying levels of damage may be identified.

The locations of sclerometric tests in the building plan, identified with the label RH (Rebound Hammer), are shown in Fig. 5.

Tests were performed by orienting the sclerometer in the horizontal direction, except in the prefabricated r.c. panels of the roof and in point RH-30-2, where the sclerometer was disposed vertically.

Since, in columns, the most severe damages were expected in the highest zones, survey spots were located at heights greater than 4 m.

A digital concrete test hammer with microprocessor was used. Cubic compressive strength were provided by the hammer from rebound indexes on the basis of correlation curves.

Rebound indexes and cubic compressive strength of concrete, R_c, based on rebound index are shown in Table 1.

4.1.2. Compression tests of drilled cores

The locations of drilled cores in the building plan, identified with label C (Core), are shown in Fig. 5.

In accordance with Italian Code [12], cores with 100 mm diameter were drilled out from spots C-30-1 and C-30-2, located in the walls. Conversely, in beams, columns and roof prefabricated panels, due to the distance between longitudinal reinforcements being less than 100 mm, concrete cylinders with 60 mm diameter were drilled.

Spot C-30-5 was chosen for the evaluation of concrete mechanical properties in undamaged structural elements. For a direct comparison between tests results on core C-30-5 and those obtained on the others

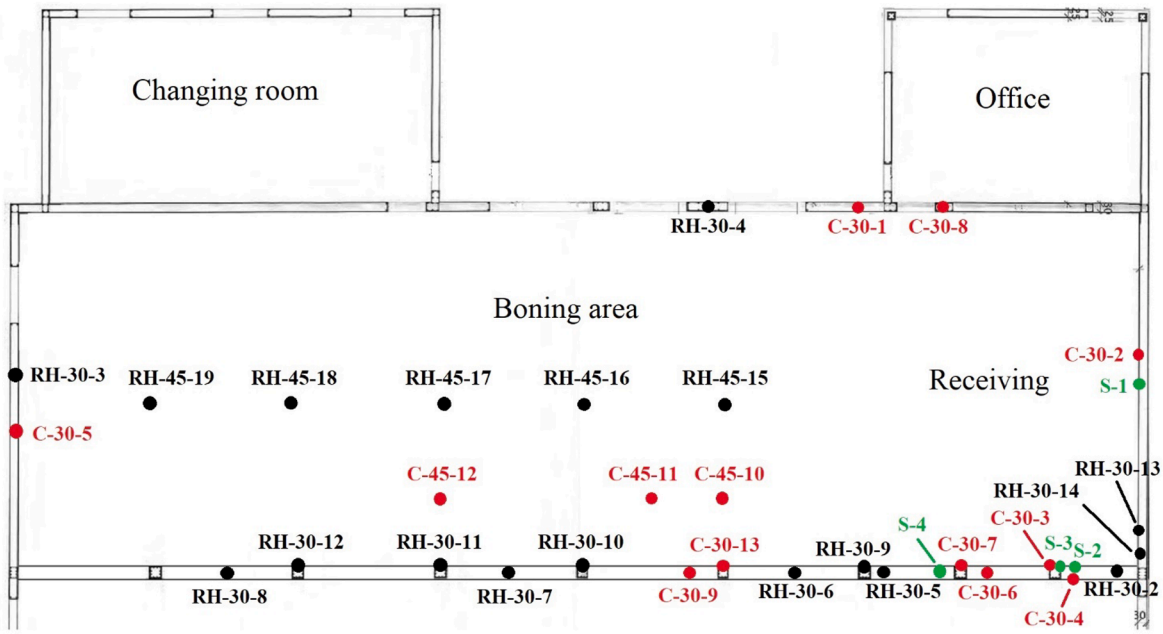

Fig. 5. Location of survey spots in the building plan for Rebound Hammer (label RH) surveys, drilled cores (label C) and reinforcement samples (label S).

Table 1
Sclerometric test results: rebound index and rebound hammer based compressive strength, R_c.

Survey spot ID	Rebound index	R_c (MPa)	Survey spot ID	Rebound index	R_c (MPa)
RH-30-1	48.6	59	RH-30-11	45.4	51
RH-30-2	26.4	8	RH-30-12	44.9	50
RH-30-3	45.5	51	RH-30-13	43.2	44
RH-30-4	47.3	56	RH-30-14	41.9	42
RH-30-5	46.9	56	RH-45-15	54.6	70
RH-30-6	47.2	56	RH-45-16	56.2	75
RH-30-7	47.8	58	RH-45-17	53.9	68
RH-30-8	47.0	56	RH-45-18	57.3	80
RH-30-9	42.6	44	RH-45-19	54.8	71
RH-30-10	49.9	66			

cores of concrete C25/30, also core C-30-5 has a diameter of 60 mm.

After drilling, cylinders were sliced into 3 parts: 2 discs, about 2.5 cm thick, and a core. Discs were obtained from the cylinder portions next to the surface exposed to fire, while the core was derived from the inner part of cylinder, adjacent to the discs.

The 2 discs derived from each cylinder were subjected to punching and indirect tensile tests, respectively, for the disc directly exposed to fire and the interior one, as described in the following. Compression tests were carried out on cores with aspect ratio l/d equal to 1.

During drilling, cylinders C-30-3 and C-30-4 were destroyed; therefore two other cylinders were extracted nearby.

Cylinders C-30-3 and C-30-7 taken from the columns, and C-30-4 and C-30-6 taken from the beams have one or more cracks crossing the longitudinal axis of the core (Fig. 6). The distance of cracks from the drilled core's surface, which was exposed to fire, ranges from 3 to 13 cm.

Damages in the cores caused by drilling, such as micro-cracking and irregularities at the drilled surface, and cutting of aggregates, are accounted for by the correction factor F_{dr} suggested by the Instructions for Italian Code implementation [13]. Values of F_{dr} suggested by [13] are reported in Table 2.

With regard to a correction factor for cores with a diameter different from 100 mm, neither the Italian Code [12] nor the Instructions [13] consider any factor. Thus, the correction factor F_{di} for cores with diameter 60 mm was derived from those proposed by ACI 214.4R-10 [14]. More precisely, in [14] F_{di} is equal to 1.06 for 50 mm diameter cores and equal to 1.00 for 100 mm diameter cores. By linear interpolation, for cores with 60 mm diameter a correction factor equal to 1.05 can be presumed.

The values of the cores' compression strength are reported in Table 3. In accordance with [13], the obtained values identify the cube strength of concrete.

4.1.3. *Punching test on discs*

For r.c. structures not affected by fire, cores compression strength is mainly determined by the concrete located in the middle third of the specimen height, since this zone is weaker than the outer thirds, which are confined from the steel plates transmitting the test load. By contrast, for structures damaged by fire, the deterioration of concrete in the outer layers exposed to fire can lead to a reduction in concrete strength that exceeds the expected increase in strength in these layers due to confining action of the steel plates transmitting the load. Thus, test results coincide with the lower strength of the concrete located in the middle third and the concrete in the damaged outer layers. Moreover, tests on cores do not account for the variability of concrete strength degradation along the specimen height as a function of the temperature range to which the concrete has been subjected. Therefore, failure stress of cores extracted from fire-damaged structures and subjected to compression are difficult to interpret. For these reasons, an equivalent compression strength of concrete was obtained from concrete flat discs, as suggested by [8]. More precisely, discs 2.5 cm thick were obtained by slicing core samples perpendicularly to the longitudinal axis. Of the 2 discs derived from each cylinder, a punching test was carried out on the disc nearest the surface exposed to fire. In this test, compression is applied to disc cores by means of two cylindrical pins of diameter 2.5 cm, at a rate of 0.4 MPa/sec. In order to reduce significantly effects due to friction between the cylindrical pins and the disc, the interface was lubricated with stearic acid. The test setup is shown in Fig. 7.

Discs subjected to the punching test were labelled similarly to the cylinders from which they are derived, substituting the C in the label with P (Punching).

Analogously to the cores' compression strengths reported in Table 3, compression strengths obtained from punching tests are modified by correction factors F_{dr} and F_{di}. The obtained values, $R_{c,p}$, are reported in Table 4.

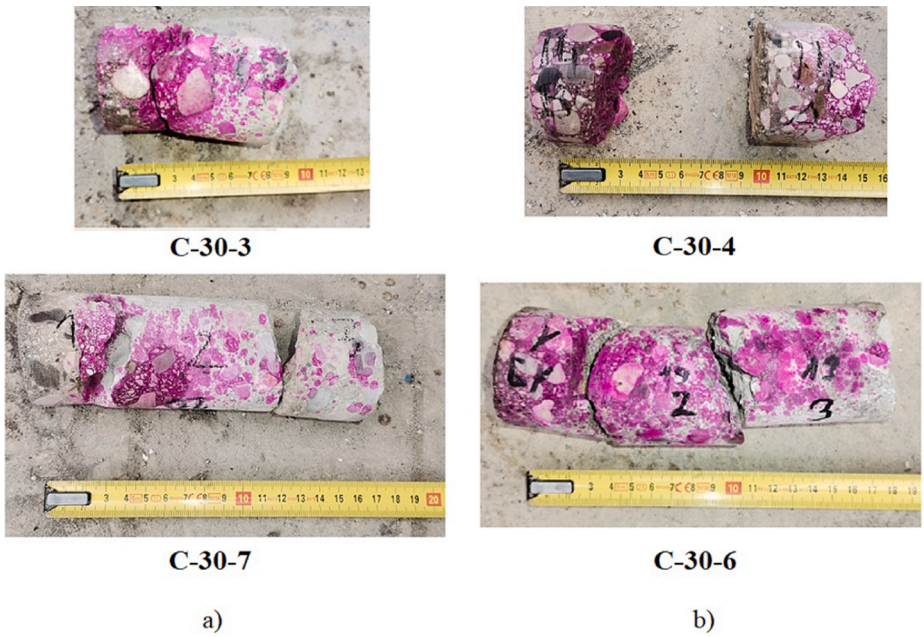

Fig. 6. Drilled cylinders with internal cracks and splits crossing the longitudinal axes of cylinders: (a) cylinders C-30-3 and C-30-7 taken from the columns, (b) cylinders C-30-4 and C-30-6 taken from the beams.

Table 2
Correction factors of core compressive strength accounting for damage due to drilling [12].

R_c (MPa)	10–20	20–25	25–30	30–35	35–40	>40
F_{dr}	1.10	1.09	1.08	1.06	1.04	1.00

Table 3
Core compressive strengths modified by correction factors F_{dr} and F_{di}, accounting for damage due to drilling and core diameter, respectively.

Core ID	Diameter(mm)	R_c (MPa)
C-30-5	60	51.9
C-30-6	60	21.3
C-30-7	60	25.5
C-30-8	60	43.7
C-30-9	60	38.1
C-30-13	60	47.4

Fig. 7. Punching test setup on concrete disc.

Table 4
Compression strength of concrete from punching tests on discs.

Disc ID	Diameter (mm)	$R_{c,p}$ (MPa)	Disc ID	Diameter (mm)	$R_{c,p}$ (MPa)
P-30-1	100	33.3	P-30-8	60	42.7
P-30-2	100	53.0	P-30-9	60	58.7
P-30-3	60	36.8	P-30-13	60	42.0
P-30-4	60	28.6	P-45-10	60	53.3
P-30-5	60	43.4	P-45-11	60	52.6
P-30-6	60	38.3	P-45-12	60	47.3
P-30-7	60	44.5			

Comparison between concrete compressive strengths of discs and cores obtained from the same cylinders is shown in Fig. 8.

4.1.4. *Indirect tensile test on discs*

The indirect tensile test method, proposed by Branco et al. [3], consists of the application of a compressive force N along a diametrical plane (Fig. 9). The splitting strength of the disc, f_{sp}, is determined by the following expression

$$f_{sp} = \frac{2N_f}{\pi dt} \tag{1}$$

with N_f the compressive force at failure, d and t the disc diameter and thickness, respectively.

As suggested by Eurocode 2 [15], the axial tensile strength of concrete, f_{ct}, may be derived from splitting tensile strength through the following expression

$$f_{ct} = 0.9 f_{sp} \tag{2}$$

Differently from [3], where discs 1.5 cm thick are considered, indirect tensile tests are carried out on discs with thickness 2.5 cm.

The discs were obtained from cylinder specimens, adjacent to the discs used for punching tests, at a depth of 2.5–5 cm. One disc for each cylinder was subjected to the indirect tensile test. Discs subjected to

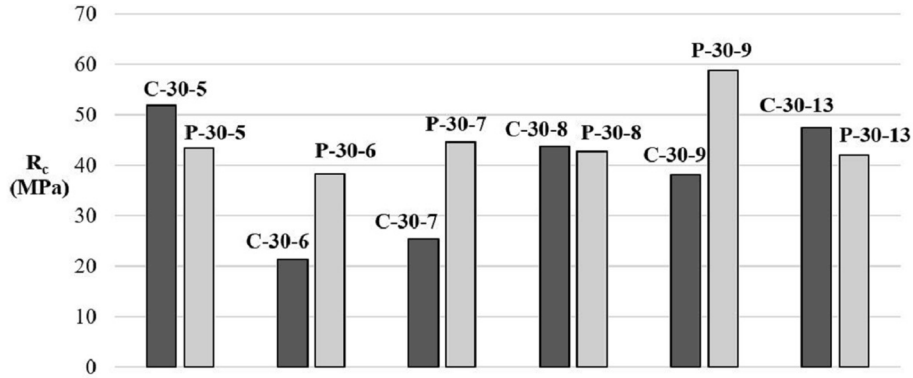

Fig. 8. Comparison between concrete compressive strengths of cores (dark grey) and discs (light grey) obtained from the same cylinders.

Fig. 9. Indirect tensile test on concrete disc.

diametrical compression are labelled similarly to the cylinders from which they were derived, substituting the C in the label with T (Tensile).

Test apparatus was conforming to European standard [16]. In particular, gaskets were made of hardboard, of density greater or equal to 900 kg/m^3, with dimensions 15 mm × 45 mm (width × length), and thickness 4 mm. Gaskets' length was chosen so to be greater than the length of the line of contact of test specimens, equal to about 25 mm. Gaskets are visible in Fig. 9.

Values of axial tensile strength obtained from discs are reported in Table 5.

4.1.5. *Carbonation test*

As outlined in [1], above 450 °C and up to 520 °C, calcium hydroxide $Ca(OH)_2$ dehydrates, decomposing into calcium oxide (CaO), which reduces the alkalinity of cement paste. Analogously to what occurs in presence of concrete carbonation, the PH reduction resulting from the temperature increase may be detected by means of a carbonation test. This test method, when it results in pink discoloration of the phenolphthalein-based solution applied to the concrete surface, may be used to highlight the depth of the 450 °C isotherm.

In fire-damaged structures, the main disadvantage of the carbonation test is that the 450 °C isotherm may be identified only in concrete samples that have not been in contact with water after fire. Water penetration in r.c. members causes rehydration of CaO, and, consequently, the reinstatement of the alkalinity of concrete, as shown in [17]. Thus, this kind of analysis is not applicable to r.c. structural elements directly exposed to water, as usually occurs when firefighters extinguish the fire, or when structural elements are exposed to rain. Moreover, the test method is not applicable even on drilled cores, since the water used for cooling the drilling tool causes $Ca(OH)_2$ reformation. Thus, the carbonation test should be performed on the pulverized concrete obtained from sorted samples during drilling.

The main disadvantage of the test method is that it is fundamental to know the carbonation depth in the structure before the fire due to normal ageing, in order to distinguish the effects of the pre-existing carbonation from those due to fire. As previously mentioned, the fire was extinguished with water, and structural elements were not protected against water. For this reason the carbonation test was not included in the test program.

Table 5
Axial tensile strength of concrete from indirect tensile tests on discs.

Disc ID	Diameter (mm)	f_t (MPa)	Disc ID	Diameter (mm)	f_t (MPa)
T-30-1	100	2.95	T-30-8	60	4.92
T-30-2	100	2.43	T-30-9	60	3.68
T-30-3	60	2.90	T-30-10	60	4.33
T-30-4	60	0.94	T-45-10	60	5.93
T-30-5	60	5.67	T-45-11	60	5.64
T-30-6	60	4.14	T-45-12	60	6.98
T-30-7	60	2.97			

4.2. *Reinforcing steel*

Results of experimental tests on various steel bars exposed to high temperatures up to 850 °C during thermal cycles [18] show that, after cooling, the Young's modulus is not influenced by the thermal treatment. Conversely, yield and ultimate steel strength and ductility are strongly affected by high temperatures. Therefore, the most important steel mechanical properties to investigate are tensile strength, at yield and ultimate conditions.

4.2.1. *Tensile test*

Four reinforcement samples were taken from the most damaged members in the receiving area, investigating all structural member typologies (i.e. beams, columns and walls). Samples about 70 cm long were obtained by cutting, by means of grinder, steel bars of structural elements, bared from the concrete cover. Then, testing samples of length 53 cm were derived for axial tensile test. Locations of steel sampling points are marked with the label S (Steel) in Fig. 5. In Fig. 10 the positions of samples S-2 and S-3 are shown. The diameters and test results of samples, i.e. yield strength, f_y, and ultimate strength and strain, f_u and ε_u, respectively, are reported in Table 6. Samples S-3 and S-4 after failure are visible in Fig. 11.

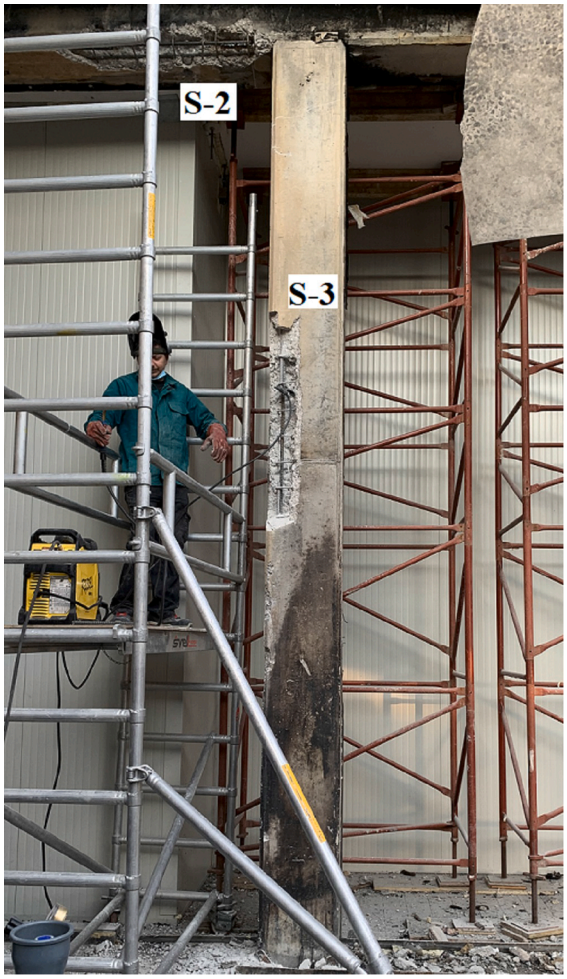

Fig. 10. Location of reinforcement samples S-2, in the beam, and S-3, in the column.

Table 6
Yield strengths and ultimate strengths and strains of steel samples from axial tensile tests.

Sample ID	Diameter (mm)	f_y (MPa)	f_u (MPa)	ε_u (%)
S-1	7.9	528	583	11.0
S-2	19.9	557	682	13.4
S-3	16.1	510	613	11.8
S-4	19.4	631	763	12.3

5. Discussion of test results

5.1. Sclerometric tests

Concrete compressive strength based on rebound hammer measurements on structural elements made of concrete C25/30 are shown in Fig. 12. From Fig. 12 it can be seen that, for the most part, strength values range from 50 MPa to 60 MPa. This data set includes survey points both far away from and near the receiving area (Fig. 5), where the most severe damage was observed. Values of concrete cubic compressive strength lower than 50 MPa were obtained only in spots RH-30-2, 9, 13 and 14, for which R_c is equal to 8, 44, 44 and 42 MPa, respectively.

By comparing the strength values obtained from walls (44 and 42 MPa) with that obtained at the end of the adjacent beam of the frame (8 MPa), it can be derived that the presence of larger amount of reinforcement strongly reduces concrete compressive strength after fire. It follows that, for buildings in earthquake zones, the greatest fire damages

Fig. 11. Reinforcement samples S-3 and S-4 after axial tensile failure.

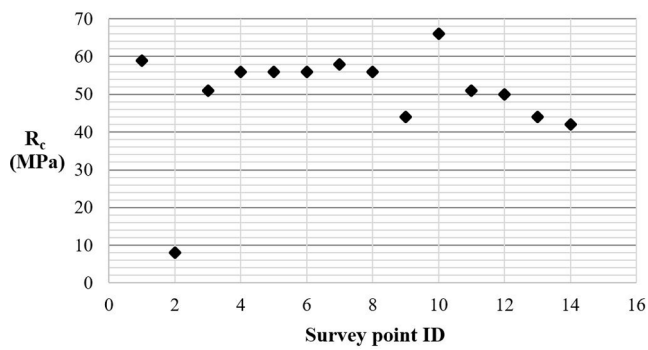

Fig. 12. Values of cube compressive strength of concrete based on rebound hammer measurements on structural elements (beams, columns and walls) made of concrete C25/30.

can be expected near the beam-column joints [19] and [20], which exhibit large amounts of reinforcements. It is pointed out that the above evidence regarding reinforcement amount has been found for the considered building, which is located in medium seismic zone (Zone 2 according to [21]). Consequently, even more severe damages are expected when fire occurs in buildings located in higher seismic risk zones.

As regards prefabricated roof panels, made of concrete C35/45, values of compressive strength derived from rebound index are presented in Fig. 13. This figure shows that strength values range from 68 MPa to 80 MPa. Moreover, it can be seen that, as sample locations move away from the receiving area towards the delivery shed (survey points from RH-45-15 to RH-45-19), the compressive strengths neither increase nor decrease in a perceptible pattern, but change randomly. Thus, it can

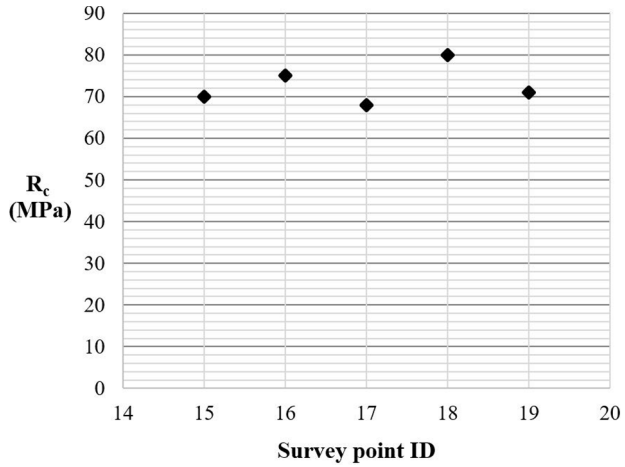

Fig. 13. Values of cube compressive strength of concrete based on rebound hammer measurements on roof prefabricated panels made of concrete C35/45.

be presumed that the roof panels over the deboning area were not damaged by fire.

5.2. Drilled cores

As previously mentioned, during drilling, cylinders C-30-3 and C-30-4 got destroyed. This is due to the weakness and friability of the concrete in the interior frame elements. Moreover, it has been observed that cylinders C-30-3, 4, 6, and 7 have one or more cracks crossing the core longitudinal axis, parallel to the core surface exposed to fire. These cracks reveal that the outer layer of concrete is separated from the inner, sound concrete, at depths ranging from 3 to 13 cm. This kind of damage, known in the literature as inner delamination [4], is due to high temperature gradients, which give rise to large tensile stresses between the outer concrete layers, affected by fire, and the cooler inner core. Moreover, some of the cracks registered on concrete cores may be connected with splitting caused by the difference between thermal deformation of reinforcing bars and that of the surrounding concrete.

It is worth to note that inner delamination, and the depth of concrete affected by this damage, cannot be detected except through concrete core drilling.

In accordance with [13], the acceptability of the cores' compressive strengths occurs for values of R_c greater than or equal to the 85% of the characteristic compressive strength associated with the strength class of concrete. Thus, for cores taken from concrete classified C25/30, compressive strength should be greater than 25.5 MPa. From Table 3 it can be seen that compressive strengths of drilled cores comply with [13], except for the strength of core C-30-6, taken from one of the interior frame beams in the receiving area (Fig. 5). Moreover, it can be observed that cores' strengths, except those of cores C-30-6 and C-30-7, are much greater than 25.5 MPa. The obtained results are consistent with the mean compressive strength of concrete cube specimens, derived from certificates of tests carried out during the construction of the building, equal to 44 MPa.

Moreover it is observed that the compressive strengths of cores C-30-5, C-30-8 and C-30-13 are higher than the nominal strength of concrete C25/30. This is probably due to the concrete aging. Sometimes the strength increment due to aging is high, as it can be seen in [20], while in other cases it is low, as deductible from the experimental data reported in [22].

5.3. Punching tests on discs

From the comparison of punching strengths of discs P-30-5, 6, 7, 8, 9, and 13 (Table 4) with the compression strengths of cores obtained from the same cylinders (Table 3), shown by Fig. 8, it can be observed that the punching strength of discs, $R_{c,p}$, exceeds the compressive strength of the corresponding core in 50% of cases. The strength increment is relevant and ranges from 35 to 44%. This result appears to be in contrast with the expectation of finding, for the outer concrete layers (those most affected by fire), strength values lower than those of the inner concrete cores. Moreover, the highest strength increment is registered in discs P-30-6 and P-30-7, taken from the frame elements that visibly appear severely damaged. This result is likely due to the confining effect of concrete surrounding the disc core subjected to axial compression, applied by the pins in the punching test. The compression strength of disc cores in absence of confinement, R_c, may be expressed as a function of the confined core compression strength in presence of the lateral confining pressure, σ_l, exerted by the surrounding concrete, $R_{c,p}$, and the compression strength increase due to σ_l, R_c^*, by the following expression

$$R_c = R_{c,p} - R_c^* \tag{3}$$

By assuming a linear elastic behavior for concrete, R_c^* may be expressed as a function of concrete longitudinal strain ε_L^* due to σ_l, by means of Hooke's law

$$R_c^* = E_{ct}\varepsilon_L^* \tag{4}$$

where E_{ct} is the concrete elastic modulus in tension.

The longitudinal strain ε_L^* is related to the compressive lateral strain ε_t^* in the concrete caused by σ_l through the following expression

$$\varepsilon_L^* = \varepsilon_t^*/\nu \tag{5}$$

where ν is the concrete Poisson's ratio.

Applying Hooke's law,

$$\varepsilon_t^* = \sigma_l/E_c \tag{6}$$

where E_c is the concrete elastic modulus in compression.

Substituting Eq. (6) in (5) and Eq. (5) in (4), the following relationship between R_c^* and σ_l is derived

$$R_c^* = \frac{E_{ct}}{\nu E_c}\sigma_l \tag{7}$$

Considering the equilibrium of the concrete hollow cylinder surrounding the disc core (Fig. 14), on which compression force is applied by pins, the following expression for σ_l is derived

$$\sigma_l = 2\frac{a}{d}\bullet\sigma_t \tag{8}$$

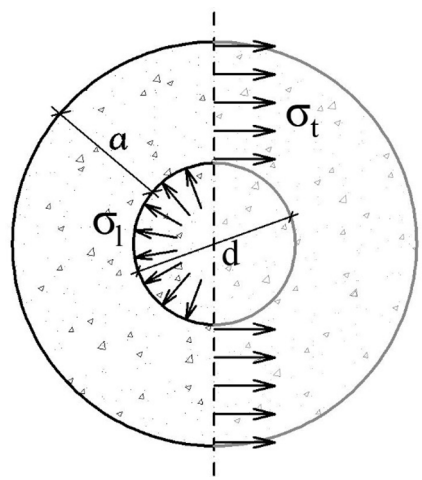

Fig. 14. Equilibrium of internal and external stresses acting on a half of the hollow cylinder surrounding the core disc subjected to axial compression.

where σ_t is the mean value of tensile stresses acting on the concrete hollow cylinder on a diametrical section plane, a is the thickness of the hollow cylinder and d the diameter of the disc core.

By assuming a uniform stress distribution on thickness a, at the attainment of tensile strength in the concrete f_{ct}, Eq. (8) becomes

$$\sigma_l = 2\frac{a}{d}\bullet f_{ct} \tag{9}$$

Substituting Eq. (9) in (7) and Eq. (7) in (3), the following expression for R_c is obtained

$$R_c = R_{c,p} - 2\frac{a}{d}\frac{E_{ct}}{\nu E_c} f_{ct} \tag{10}$$

Eq. (10) shows that the compression strength of disc cores in absence of confinement, R_c, may be calculated by subtracting from $R_{c,p}$ the strength contribution due to confinement, which depends on the mechanical properties of concrete.

It has been demonstrated that confinement contribution depends on E_{ct}, E_c, ν, and f_{ct}.

For fire-damaged concrete, these properties depend on the temperatures achieved in the concrete during the fire. If the profile of temperatures in the concrete while exposed to fire is estimated, the parameters E_{ct}, E_c, and f_{ct} may be calculated from the temperature data and the mechanical properties of the undamaged concrete using formulas available in the literature, such those reported in [23] and [24]. However, there is little data available about Poisson's ratio at high temperatures, and the literature indicates that Poisson's ratio does not have a strong dependence on temperature, as outlined in [24].

In the light of the foregoing, punching test results are difficult to interpret and, above all, it is hard to derive from them the compressive strength of damaged concrete.

5.4. Indirect tensile tests

In this study it is considered that axial tensile strengths of concrete must comply with Italian Code [12] when greater than or equal to the characteristic (95% fractile) axial tensile strength, f_{ctk}, of the concrete strength class. According to [12], f_{ctk} is set equal to 70% of the average tensile strength, f_{ctm} ; that is

$$f_{ctk} = 0.7 f_{ctm} \tag{11}$$

and f_{ctm}, for concrete of strength class lower than C50/60, is related to the characteristic value of cylindrical compressive strength, f_{ck}, as follows

$$f_{ctm} = 0.3(f_{ck})^{2/3} \tag{12}$$

Thus, for discs of concrete C25/30, the obtained axial tensile strengths should be greater than 1.80 MPa, and, for discs of concrete C35/45, greater than 2.25 MPa.

From Table 5 it can be seen that all axial tensile strengths of the tested discs comply with [13], except for T-30-4, taken from the interior frame beam, in the receiving area, which, from visual assessment, appeared the most damaged.

It should be noted that the tensile strengths of discs T-30-3, 6 and 7, taken from other elements of the frame that appeared severely damaged, fulfil the requirement. This result is in contrast with the expectation of finding, for discs T-30-3, 6 and 7, strength values lower than 1.80 MPa, having determined that the concrete was weak and friable in these zones. It may be surmised that the concrete tensile strengths derived from tests on these discs is not reliable, probably due to the small thickness of discs, which is similar to the aggregate size. However, the test method may be performed on subsequent discs obtained from the same cylinder, to determine the depth in the member cross-section at which the concrete tensile strength stabilizes. In this way, an estimation of the thickness of the damaged concrete layer might be determined.

5.5. Axial tensile tests on reinforcing steel

Steel tensile strengths obtained from tests are considered adequate when greater than the characteristic strengths prescribed by Italian Code applicable at the time of building construction [21] for steel grade FeB 44 k. More precisely it is checked that f_y, and ultimate tensile strength, f_u, obtained from testing are higher than the characteristic (fractile 95%) values of yield strength, f_{yk}, and ultimate strength, f_{uk}, respectively. According to [21], f_{yk} and f_{uk} are equal to 430 MPa and 540 MPa, respectively.

From Table 6 it can be seen that all tested samples satisfy the minimum strength requirements of the Italian Code, used in structural verifications.

Moreover, the obtained results are consistent with the mean values of yield and ultimate strengths derived from tests certificates provided by the manufacturer, respectively equal to 549 MPa and 650 MPa.

As regards the acceptability of the ultimate strain, ε_u, provisions given in [21] cannot be applied, since they refer to strains measured in the start of the necking region. Conversely, values of ε_u reported in Table 6 are measured far away from the necking region, as required by current Code [12].

Since steel of quality FeB 44 k is very similar to steel B450C, it is checked that values of ε_u are higher than the characteristic (fractile 95%) value of ultimate strain, ε_{uk}, prescribed by technical standards [12] for steel B450C, equal to 7.5%. MPa. From Table 6 it can be seen that all tested samples satisfy the strain requirement. Thus, steel reinforcements are considered to be adequate.

6. Proposed repair intervention

On the basis of experimental results of in situ and laboratory tests and the data obtained during visual inspection of the structure, it is concluded that repair interventions should be performed on columns and beams in the first three bays of the central frame in the receiving area. Moreover, repairs are required on the wall in the receiving area adjacent to the interior frame, over on area of about 3×3 m^2.

The continuity of the existing steel bars, from which steel samples were extracted, was restored by welding to them bar pieces of the same diameter. Also the concrete cover was restored with anti-shrinkage grout.

In order to restore the load-bearing capacities of structural elements damaged by fire, to their condition prior to the fire, the following repair interventions are proposed.

(1) Demolition of the roof over the receiving area and of rods on the contour in order to ensure the anchoring of the new roof to the existing structure.
(2) Removal of the outer concrete up to a depth of about 3–5 cm at the extrados of the central beams adjacent to the demolished roof portion, preserving beams' reinforcements.
(3) Horizontal drillings in the central beams up to a depth of 60 cm, in order to create the holes to anchor the new lower reinforcements of the roof portion to be restored.
(4) Demolition of the topping concrete of the roof over the curing department, for a length of 20 cm, to embed the new upper longitudinal reinforcements, crossing the supporting beam, in order to connect adequately the new roof with the existing one. The new reinforcements overlap to those of the existing roof for a length equal to the beam width plus the 20 cm length of demolition.
(5) Replacement of the roof panels with panels with the same load-bearing capacity, and restoration of the steel reinforcements.
(6) Filling of the holes in the central beams with anti-shrinkage grout.

(7) Restoration of the concrete at the extrados of the central beams and the topping of the roof over the curing department with anti-shrinkage grout.
(8) Removal of the damaged concrete outer layers from columns and beams, down to the sound core, and installation of additional stirrups, in order to confine the concrete core affected by internal cracks, due to inner delamination; restoration of the concrete cover with anti-shrinkage grout, by increasing members' cross-sections of about 2 cm on each side.
(9) Removal of the damaged concrete cover from the deteriorated area of the wall down to the sound concrete layers, and restoration of the concrete cover with anti-shrinkage grout.
(10) Restoration of the completion concrete of the roof and the contouring rods.
(11) Restoration of installations, finishes and non-structural elements damaged by fire.

7. Conclusions

The proposed case study is useful to highlight advantages and limitations of the adopted test methods.

In light of the results obtained from the test program and the information captured during visual inspection of the r.c. structure the following conclusions can be drawn:

(1) Visual assessment of the structure is fundamental to identify the most fire-damaged members and, thus, to calibrate the test program, determining the locations of survey points.
(2) The detection of pink-red discoloration on the surface concrete of structural members up to a depth of about 3–4 cm in the cross-section is useful for an approximate estimation of the penetration of heating and of the concrete thickness subjected to temperatures between 300 °C and 600 °C.
(3) Sclerometric tests are useful for mapping the damage distribution in the structure. By considering a sufficient number of survey points, both far away from and near the most damaged area, and comparing values of rebound index, zones with varying levels of damage can be identified. In the present case it was found that, for a great part, strength values range from 50 MPa to 60 MPa and only in the elements most exposed to fire values of concrete cubic compressive strength lower than 50 MPa were obtained.
(4) Cracks crossing the longitudinal axis of concrete cylinders, parallel to the surface exposed to fire, reveal inner delamination, i.e. the separation of the outer layer of concrete from the inner concrete. This damage is due to high temperature gradients. Moreover, some of cracks on concrete cores can be connected with splitting caused by the difference between thermal deformation of reinforcing bars and that of the surrounding concrete.
(5) Results of punching test results on thin discs are influenced by the confining effect of concrete surrounding the disc core being subjected to axial compression applied by pins. In the present case it was found that, in the elements which appeared the most damaged by fire, the punching strengths of discs were higher than the compressive strengths of cores cut from the same cylinders, in the interior part. It has been shown that it is hard to quantify the confinement contribution and, therefore, to determine the residual strength of damaged concrete in absence of confinement.
(6) In structural elements with small diameter and well-spaced reinforcements cracks due to difference between thermal deformation of reinforcements and that of the surrounding concrete are much less numerous and less open than in strongly reinforced elements. In the present case test results have shown little damage in the wall in the receiving area close to the ignition point of the fire, although the interior frame members near the wall were severely damaged. It can be surmised that in strongly reinforced zones, as beam-column joints, the greatest fire damaged can be expected. An important and original conclusion of this work is that, after a fire, the concrete strength at beams and columns ends and in beam-column joints should be investigated.
(7) In the restoration of the load-bearing capacity of the building to the condition existing prior to the fire, to ensure the anchoring of the new roof to the existing structure, the rods on the roof contour were demolished and restored.
(8) To connect adequately the new roof with the existing one, the topping concrete of the existing roof was demolished for a length of 20 cm, in order to increase the embedment length of the new upper longitudinal reinforcements.
(9) Installation of additional stirrups in columns and beams is useful to confine the concrete core affected by inner delamination.

CRediT authorship contribution statement

Giada Frappa: Conceptualization, Methodology, Formal analysis, Investigation, Writing – original draft, Writing – review & editing. **Margherita Pauletta:** Formal analysis, Investigation, Data curation. **Caterina Di Marco:** Investigation, Data curation, Visualization. **Gaetano Russo:** Conceptualization, Methodology, Resources, Writing – review & editing, Project administration, Supervision.

Declaration of Competing Interest

The authors declare that they have no known competing financial interests or personal relationships that could have appeared to influence the work reported in this paper.

References

[1] Tattoni S. Metodi di indagine sulle strutture (strutture in ca dopo l'evento incendio). In: International Seminar "Evoluzione nella Sperimentazione per le Costruzioni", Centro Scientifico Internazionale di Aggiornamento Sperimentale-Scientifico. Spain, Madrid; 8-15 may 2010:191-216.
[2] Wróblewska J, Kowalski R. Assessing concrete strength in fire-damaged structures. Constr Build Mater 2020;254:119122. https://doi.org/10.1016/j.conbuildmat.2020.119122.
[3] dos Santos JR, Branco FA, de Brito J. Assessment of concrete structures subjected to fire - The FBTest. Mag Concr Res 2002;54(3):203–8.
[4] Malešev M, Radonjanin V. Fire damages of reinforced concrete structures and repair possibilities. Knowledge FOr Resilient soCiEty K-FORCE 2019.
[5] Di Luzio G, Muciaccia G, Biolzi L. Size Effect in Thermally Damaged Concrete. Int J Damage Mech 2010;19(5):631–56.
[6] Cattaneo S, Biolzi L. Assessment of Thermal Damage in Hybrid Fiber-Reinforced Concrete. J Mater Civ Eng 2010;22(9):836–45.
[7] Di Luzio G, Biolzi L. Assessing the residual fracture properties of thermally damaged high strength concrete. Mech Mater 2013;64:27–43.
[8] Benedetti A, Mangoni E. Damage assessment in actual fire situations by means of non-destructive techniques and concrete tests. In: 2nd Fib Task Group 4.3 Workshop "Fire Design of Concrete Structures: In: What Now? What Next?". Italy, Milan; 2-4 Dec 2004.
[9] Hager I. Behaviour of cement concrete at high temperature. Bull Polish Acad Sci: Tech Sci 2013;61(1).
[10] Short NR, Purkiss JA, Guise SE. Assessment of fire damaged concrete using colour image analysis. Constr Build Mater 2001;15(1):9–15.
[11] Wald F, Burgess I, Annerel E, Taerwe L. Assessment techniques for the evaluation of concrete structures after fire. J Struct Fire Eng 2013;4(2):123–30.
[12] Ministero delle Infrastrutture e dei Trasporti. DM 17 gennaio 2018. Norme tecniche per le costruzioni; 2018 [in Italian].
[13] Consiglio Superiore dei Lavori Pubblici. Circolare 21 gennaio 2019, n. 7 - Istruzioni per l'applicazione dell'«Aggiornamento delle "Norme tecniche per le costruzioni"» di cui al decreto ministeriale 17 gennaio 2018; 2018 [in Italian].
[14] ACI Committee 214.4R-10. Guide for Obtaining Cores and Interpreting Compressive Strength Results. Farmington Hills; American Concrete Institute; Michigan, 2010 (Reapproved 2016).
[15] UNI EN 1992-1-1:2005. Eurocode 2: Design of concrete structures - Part 1: General rules and rules for buildings. CEN, Comité European de Normalisation; 2004.
[16] UNI EN 12390-6:2010. Testing hardened concrete - Part 6: Tensile splitting strength of test specimens. CEN, Comité European de Normalisation; 2010.
[17] Li Q, Zhuguo L. Repair of Fire-Damaged Concrete: Improvement of Carbonation Resistance. In: Second International Conference on Sustainable Construction Materials and Technologies. Italy, Ancona; 28–30 June 2010:1557–67.

[18] Yao X, Qin P, Guan J, Li L, Zhang M, Gao Y. Residual Mechanical Properties and Constitutive Model of High-Strength Seismic Steel Bars through Different Cooling Rates. Materials 2021;14(2):469. https://doi.org/10.3390/ma14020469.
[19] Pauletta M, Di Marco C, Frappa G, Somma G, Pitacco I, Miani M, et al. Semi-empirical model for shear strength of RC interior beam-column joints subjected to cyclic loads. Eng Struct 2020;224:111223. https://doi.org/10.1016/j.engstruct.2020.111223.
[20] Pauletta M, Di Marco C, Frappa G, Miani M, Campione G, Russo G. Seismic behavior of exterior RC beam-column joints without code-specified ties in the joint core. Eng Struct 2021;228:111542. https://doi.org/10.1016/j.engstruct.2020.111542.
[21] Ministero dei Lavori Pubblici. Decreto Ministeriale 9 gennaio 1996. Norme tecniche per il calcolo, l'esecuzione ed il collaudo delle strutture in cemento armato, normale e precompresso e per le strutture metalliche; 1996 [in Italian].
[22] Shannag MJ, Higazey M. Strengthening and Repair of a Precast Reinforced Concrete Residential Building. Civil Eng J 2020;6(12):2457–73.
[23] Bastami M, Aslani F, Esmaeilnia OM. High-Temperature Mechanical Properties of Concrete. International. J Civil Eng 2010;8(4).
[24] Naus DJ. Compilation of Elevated Temperature Concrete Material Property Data and Information for Use in Assessments of Nuclear Power Plant Reinforced Concrete Structures. Washington, D.C.: U.S. Nuclear Regulatory Commission, Office of Nuclear Regulatory Research; 2010.